# A Fast Self-calibration Method for Piezoelectric Sensors Excited by Pseudorandom M-sequence

Zhaoyu Zhang, Tianyi Shi, Luca Lombardo, *Member, IEEE*, Yidan Hu, Haotian Wang, Xuanrui Zhang, Marco Parvis, *Fellow, IEEE*, and Junhao Li, *Senior Member, IEEE*

***Abstract*—Piezoelectric element is the most critical component of a piezoelectric sensor, commonly applied for defect detection of electrical equipment. To ensure the sensor work stably and reliably, impedance and sensitivity response curves should be calibrated periodically with specific technical platforms in laboratory to evaluate the sensor's performance and characteristics. This is costly, time-consuming and inconvenient for industrial measurements. Pseudorandom M-sequence is a kind of binary signal that exhibits statistical characteristics similar to white noise. This paper proposes a fast self-calibration method based on pseudorandom M-sequence, which is suitable for acquiring the impedance and sensitivity response curves of piezoelectric sensors. The clock pulse frequency of M-sequence can be adjusted to match the calibration band. The simulation and experimental results confirm that this method is feasible, reliable and efficient in terms of both power and time consumption, requiring a few milliseconds and approximately 10 mW for a single calibration. The method was successfully applied in a commercial AE sensor and a recently-developed wireless piezoelectric sensor. This work provides a novel solution for the self-calibration of smart piezoelectric sensors.**

***Index Terms*—self calibration, smart wireless sensor, piezoelectric sensors, impedance and sensitivity response curves, pseudorandom M-sequence.**

## I. Introduction

Piezoelectric transducers are extensively applied in industrial measurement and energy conversion because of their good stability, performance and high efficiency. Specifically, piezoelectric acoustic emission (AE) sensors could be used to capture partial discharge (PD) signals in power equipment for insulation evaluation [1], or to find the exact location of the source of bearing damage for material evaluation [2]. Similarly, piezoelectric vibration sensors perform well at detecting mechanical defects in power equipment such as transformers and induction motors [3]-[5], while piezoelectric transformers are prominent components in many power devices [6], [7]. The piezoelectric element, such as lead zirconate titanate (PZT) and piezoelectric polymers, are key components of the piezoelectric sensors which performance is influenced by environment, operating duration and structure itself [8], [9]. Any change in sensor performance parameter could cause inaccuracy of the measurement. Therefore, it is necessary to calibrate the piezoelectric sensors periodically.

The impedance curve and sensitivity curve in frequency domain are two important parameters of any piezoelectric sensor, reflecting the electrical response and mechanical response respectively, both of the two curves should be calibrated properly before any measurement [10], [11]. Generally, the impedance curve of piezoelectric sensor is measured by impedance analyzer with sweep frequency method, while the sensitivity curve of piezoelectric sensor is calibrated on specific platforms employing several devices. Take piezoelectric vibration sensor calibration (working under 2 kHz) as an example in Fig. 1. It is advised that the Sensor Under Test (SUT) and the Reference Sensor (RS, whose sensitivity curve is known) are fixed face-to-face on a vibration exciter supplied by a suitable power amplifier and controlled by a frequency generator. Then, the SUT could be calibrated with RS by sweep frequency vibration [12].

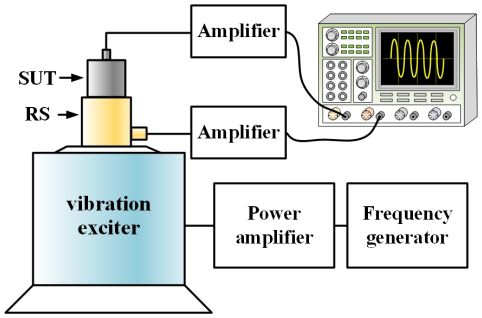


Fig. 1. Typical sensitivity calibration setup for piezoelectric vibration sensors.

In addition, the calibration test of piezoelectric AE sensor is also inconvenient, the two common methods are surface pulse calibration and reciprocity calibration [13], respectively seen in Fig. 2 (a) and (b). For surface pulse calibration, the SUT and the RS are placed in opposite direction at equal distance (10 cm) from the pencil-lead-break source which is put at the center of a 42 cm diameter and 21 cm height steel block. The signals from the two sensors are acquired and processed to complete the calibration [14]. In order to achieve the best calibration accuracy, the RS should be replaced by a high-performance

Manuscript received xxx; revised xxx; accepted xxx. This work was supported by National Natural Science Foundation of China Joint Fund Key Project under Grant U22B20118. *(Corresponding author: Junhao Li.)*

Zhaoyu Zhang, Tianyi Shi, Yidan Hu, Haotian Wang, Xuanrui Zhang and Junhao Li are with the State Key Laboratory of Electrical Insulation and Power Equipment, Xi'an Jiaotong University, Xi'an 710049, China (e-mail: junhaoli@mail.xjtu.edu.cn).

Zhaoyu Zhang, Luca Lombardo and Marco Parvis are with the Department of Eletronics and Telecommunications, Politecnico di Troino, 10129 Turin, Italy

capacitive displacement transducer [15]. There are two key factors which are challenging in surface pulse calibration: acquiring stable and reliable acoustic source as well as measuring the exact displacement of surface. Therefore, to avoid measuring the surface acoustic signals such as displacement or velocity, reciprocity calibration can be employed which only requires electric signals [16]. According to the electroacoustic reciprocity characteristic of AE sensors, the transmitting current response and receiving voltage response are measured to calculate the acoustic transfer impedance (usually called reciprocity constant). In Fig. 2 (b), three similar AE sensors are needed and two of them are installed every time, S1 transmits and S2 receives; S2 transmits and S3 receives; S3 transmits and S1 receives, then the sensitivity of S1 could be obtained by solving the reciprocity equation [17].

In conclusion, not only the calibration tests of piezoelectric sensors are extremely time-consuming, but also they are expensive and require bulky dedicated equipment, which means the tests can only be implemented in laboratory.

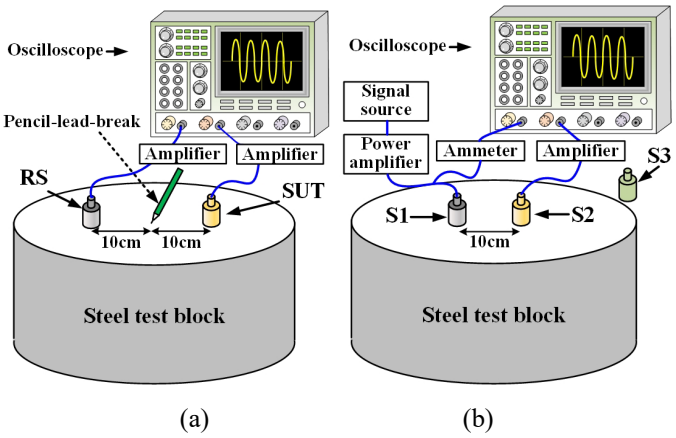


Fig. 2. The sensitivity calibration setups for piezoelectric AE sensor. (a) Surface pulse calibration. (b) Reciprocity calibration.

To improve the efficiency of piezoelectric sensor sensitivity on-site calibration, Hua Lan et al. proposed in [18] a surface-to-surface method to obtain the sensitivity response of AE sensors point by point, the results are consistent with that measured by ISO standards. But this is not suitable for field tests because it requires some bulky devices such as wave generating board and oscilloscope. Lu Zhang et al. realized the absolute calibration of piezoelectric AE sensors through multi-physics numerical and experimental models. However, the practical parameters of electrical models can be acquired difficultly and the result precision needs to be improved [19]. Therefore, present calibration methods of piezoelectric sensors are not convenient and efficient for multi-sensor calibration especially either in urgent cases or on-field applications

Nowadays, under the fourth industrial revolution, sensing technology is evolving to be distributed, multi-signal, smart, and wireless with low energy requirements [20], [21]. Thus, self-calibration obtains attention of researchers as an essential feature of smart sensors, assuring the proper working and the required measurement accuracy [22]-[24] over a long time. The self-calibration is an operation that, at application site, the sensor establishes a relation between the quantity values of the measured item and the corresponding indications primarily through its internal system configuration. Though absolute self-calibration is extremely difficult and cannot completely take place of international standards, conditional self-calibration could efficiently reflect the performance change of the sensors and extend the time between (re)calibrations in laboratory [25]. Economically, the cost of calibration is reduced significantly. Quickly and efficiently, each sensor could be calibrated by embedded devices. Technically, by adopting a self-calibration approach, it is possible to monitor the condition of the measuring devices, ensuring the accuracy of information about the measured objects. The existing studies integrate actuator inside the sensor for self-calibration, but they require external power source and data acquisition system [26], which is still costly and inconvenient, and the accuracy would decrease due to the inside actuator change. There are a few reports about the self-calibration applied on piezoelectric sensors.

With the aim of improving the electrical equipment measurement automation, this paper presents a self-calibration method excited by pseudorandom Maximum-length linear feedback shift register sequence (M-sequence), which could realize fast measurement of impedance and sensitivity response curves of the piezoelectric sensors. M-sequence is introduced and the parameters of excitation signal is theoretically determined. Simulations on circuit and Finite Element Analysis (FEA) are carried out to verify the feasibility of proposed method. Furthermore, the method is applied both on a commercial AE sensor and a recently-developed smart wireless sensor. The experimental results demonstrate its advantage in cost, time and efficiency, making it highly suitable for distributed multi-sensor on-field calibration. This method would also be effective in other applications for impedance and sensitivity response calibration.

## II. Sensing Principle and Simulation

### A. The Sensing Principle

Piezoelectric transducer is able to make conversion between electrical and mechanical energy, the output would be voltage variation if the input is mechanical variation, and vice versa. The electrical equivalent circuit of the piezoelectric sensor is shown in Fig. 3 [10]:

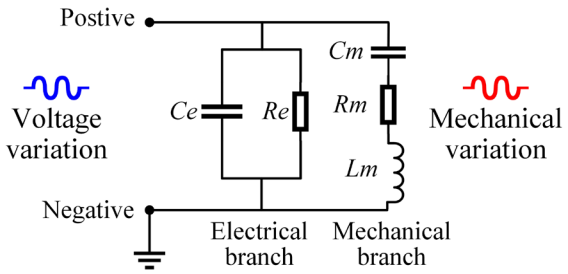


Fig. 3. The electrical equivalent circuit of a generic piezoelectric sensor.

where $R_m$, $L_m$ and $C_m$ represent the mechanical branch reflecting the sensitivity curve, while $R_e$ and $C_e$ represent electrical branch of the impedance curve. The two curves are important for confirming the sensor performance and characteristics.

### B. The Pseudorandom M-sequence

Although white noise is the ideal excitation signal for calibration since its power spectral density distributes uniformly over the entire frequency band, it can be generated difficultly and typically requires high-end expensive and bulky equipment. However, pseudorandom binary M-sequence, a periodic sequence owing similar statistical properties with discrete binary white noise, makes it possible to calibrate frequency response curve quickly [27]. The advantages of M-sequence are prominent, it can be designed by linear feedback shift register, and generated by a low-cost Digital-to-Analog Converter (DAC), so it has good repeatability; the measurement band can be set up easily by adjusting the clock frequency of the M-sequence; and most importantly, the whole measurement takes a very short time (some milliseconds) and a few power.

M-sequence could be designed by a set of binary linear feedback shift registers ($R_i$, $i$ = 1, 2, **…** $n$) with XOR operations as reported in Fig. 4 (a). $C_i$ is set as 1 or 0 to control if the register $R_i$ participates in feedback, this would determine structure and link of the sequence. Besides, $x_i$ is the state of $R_i$.

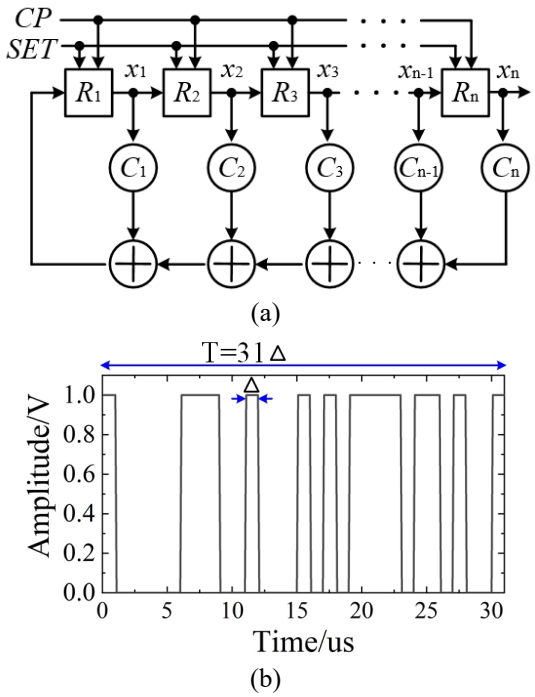


Fig. 4. The generation of M-sequence. (a) Binary linear feedback topology for generating M-sequence. (b) Example of a period of 5-stage M-sequence signal.

According to Fig.4 (a), the feedback function is:

$$F(x_1, x_2, \cdots x_n) = C_1 x_1 \oplus C_2 x_2 \oplus \cdots \oplus C_n x_n \quad (1)$$

where $\oplus$ represents the XOR operator. Except for the full zero state, there are in total $N_p$=$2^n$ - 1 states for the $n$-stage shift registers, which makes up a specific period sequence. If $\Delta$ is a duration of one stage, then the maximum period of an M-sequence should be $T$=$N_P$ • $\Delta$. An example of 5-stage M-sequence is shown in Fig. 4 (b). The eigenpolynomial of $C_i$ should be:

$$f(x_1, x_2, \cdots, x_n) = C_0 + C_1 x^1 + C_2 x^2 + \cdots C_n x^n = \sum_{i=0}^{n} C_i x^i \quad (2)$$

where $C_0$ = $C_n$ = 1, and $x$ does not have practical meaning. To generate an M-sequence similar with white noise, the eigenpolynomial must be primitive polynomial which ensures the generated sequence is a maximum length sequence with good random properties [27]. Besides, the $N_p$ should be large. It is explored that 11-stage M-sequence is suitable for our application, so the $N_p$ equals 2047. The minimum primitive polynomial and the corresponding feedback function are:

$$f(x_1, x_2, \cdots, x_n) = 1 + x^2 + x^{11} \quad (3)$$

$$F(x_1, x_2, \cdots, x_n) = x_2 \oplus x_{11} \quad (4)$$

The measurement bandwidth $f_m$ of M-sequence could be calculated by Eq. (5), where $f_{cp}$ is the frequency of clock pulse ( $\Delta$ )[28].

$$f_m \approx \frac{f_{cp}}{3} = \frac{1}{3 \cdot \Delta} \quad (5)$$

Generally, the Partial Discharge (PD) characteristic band in Gas Insulated Switchgear (GIS) involves frequency component from 20 kHz to 100 kHz [29], which is chosen as the measurement band in this paper. So the $f_{cp}$ should be 300 kHz ( $\Delta \approx 0.33\,\mu s$ ). Therefore, a period of M-sequence signal would be of only 6.823 ms. Fig. 5 describes the normalized power spectrum of 11-stage M-sequence signal when $f_m$=100 kHz and $f_{cp}$=300 kHz.

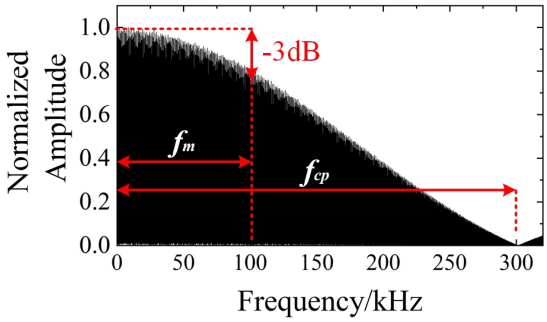


Fig. 5. The power spectrum (normalized) of 11-stage M-sequence in frequency domain when $f_m$=100 kHz.

### C. The simulation

Although the impedance and sensitivity response curves share the same measurement principle, they are slightly different regarding the measurement topology. Fig. 6 (a) and (b) describe primary measurement topologies in which the SUT is considered as two-port network, while the input could be a M-sequence or a sweep frequency signal. For impedance response measurement, a matching resistor (50 Ω) is required to connect in series with the SUT. However, for sensitivity measurement, the mechanical variation of RS generated by input signal (piezoelectric effect) is applied to the SUT, which means they are installed surface to surface with coupling

agent. In both the two cases, the voltage at the output of the SUT is acquired for performing the calibration.

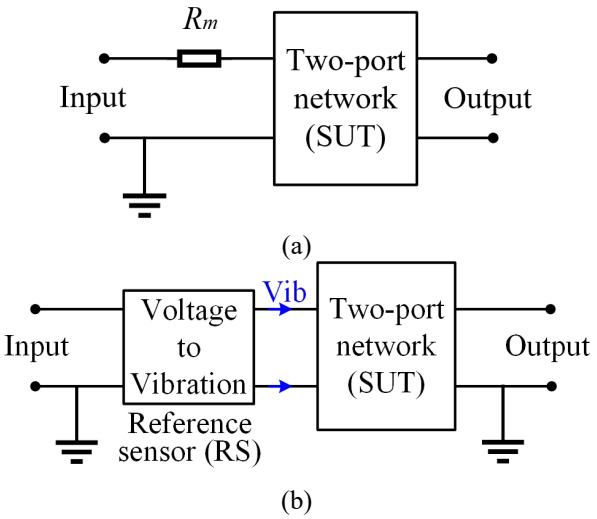


Fig. 6. Measurement topologies. (a) Impedance response measurement topology. (b) Sensitivity response measurement topology.

Finally, impedance and sensitivity response curves $Z(f)$ and $S_{SUT}(f)$ could be calculated by Eq. (6) and Eq. (7) respectively, where $f$ is the frequency, $R_m$ stands for matching resistor (50 Ω), $U_{out}(f)$ and $U_{in}(f)$ represent respectively the voltage amplitudes at the output and input, while $T_{RS}(f)$ is the transmitting sensitivity response of the RS.

$$Z(f) = R_m \frac{U_{out}(f)}{U_{in}(f) - U_{out}(f)} \tag{6}$$

$$S_{SUT}(f) = 20 \times \log_{10} \frac{U_{out}(f)}{U_{in}(f)} + T_{RS}(f) \tag{7}$$

The equivalent circuit for impedance curve simulation is shown in Fig. 7 (a). $R_e$ (5 MΩ) and $C_e$ (8 nF) are described in Fig. 3. The signal source is set by the M-sequence signal or the sweep frequency signal. The comparative result is shown in Fig. 7 (b). Hereby, Variance Analysis Factor (VAF) R-Square is used to describe the similarity between two curves, as shown in Eq. (8), Eq. (9), Eq. (10):

$$SS_{tot} = \sum_i (y_i - \bar{y})^2 \tag{8}$$

$$SS_{res} = \sum_i (y_i - z_i)^2 \tag{9}$$

$$R^2 = 1 - \frac{SS_{res}}{SS_{tot}} \tag{10}$$

where $SS_{tot}$ and $SS_{res}$ represent total sum of squares and residual sum of squares respectively, $y_i$ and $z_i$ are the ith sample of the two arrays respectively, and $\bar{y}$ is the mean of $y$ array. $R^2$ is the R-Square parameter, the closer $R^2$ is to 1, the more similar the two arrays are. In this case, the $R^2$ equals to 0.994, demonstrating that M-sequence method is as accurate as sweep frequency method.

As for sensitivity response curve, it is actually electromechanical response calibration (piezoelectric effect), so FEA is more appropriate than circuit simulation. Simulation

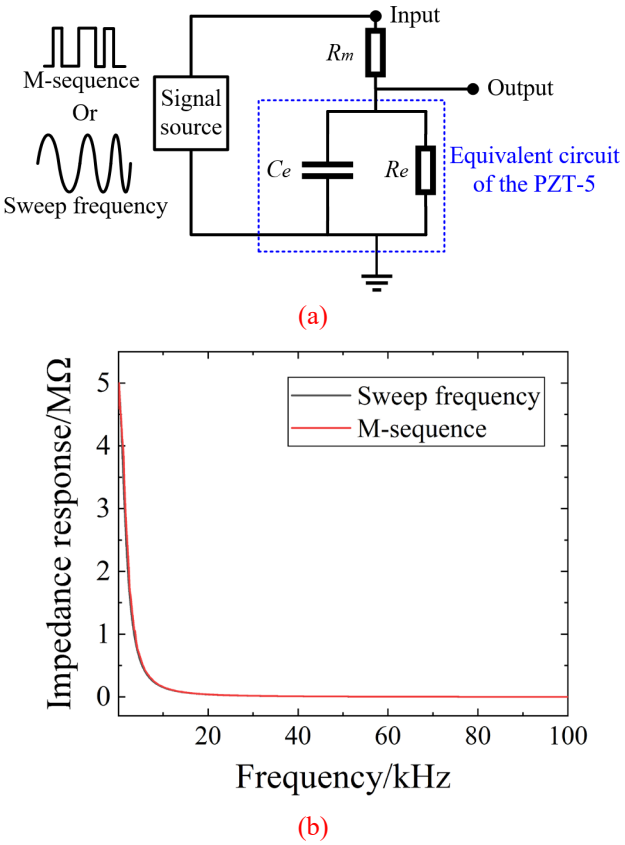


Fig. 7. Electric circuit simulation. (a) Simulation circuit for measuring impedance curve. (b) Impedance curves measured by M-sequence and sweep frequency methods.

structure is illustrated in Fig. 8 (a). The piezoelectric coupling module is applied on the PZT-5, the static and solid mechanics modules are applied on PZT-5 and metal. The bottom PZT-5 element serves as the RS which converts the input voltage signal (M-sequence or sweep frequency) to vibration as the excitation source. The upper PZT-5 element and the middle metal layer represent the SUT (the metal could be either the matching layer or the base of piezoelectric sensor), the metal is grounded. Finally, the output voltage on the top can be captured when the simulation is done. The simulation employed with M-sequence method is carried out in transient study step, while the one with sweep frequency method runs in frequency domain study step. The simulation setup is demonstrated in TABLE I.

TABLE I
THE FEA SIMULATION SETUP

| | |
|---|---|
| **Material & Dimension** | PZT-5: 4 mm height, 20 mm diameter<br>Copper: 4 mm height, 24 mm diameter |
| **Input voltage** | M-sequence or Sweep frequency signal with the same 1 V amplitude. |
| **Static and solid mechanics modules** | PZT-5, Copper |
| **Piezoelectric coupling module** | PZT-5 |

According to Eq. (7), the sensitivity response curves measured by the two methods can be calculated and shown in

Fig. 8 (b), they coincide very well, in this case, the $R^2$ is 0.9929.

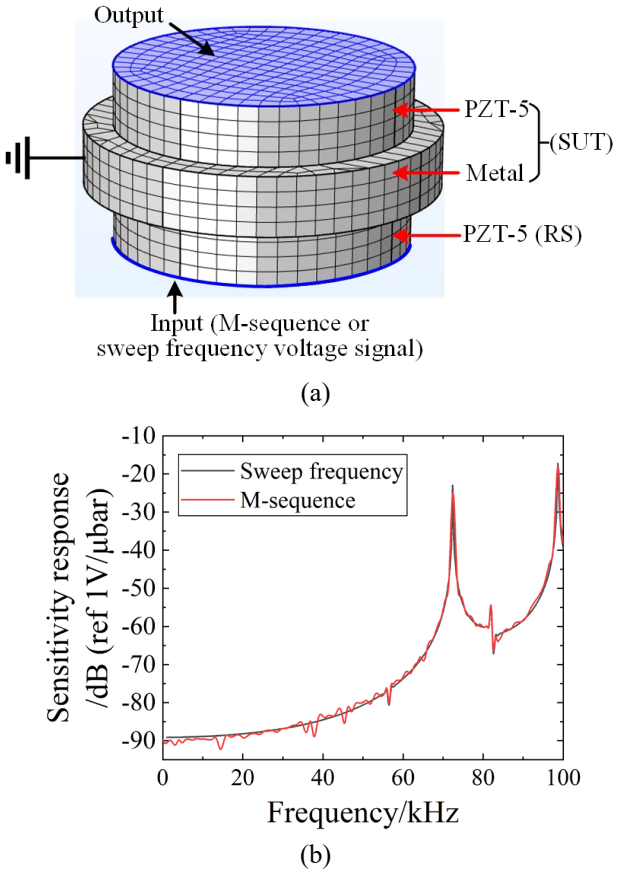


Fig. 8. FEA simulation. (a) FEA simulation set up. (b) Sensitivity response curves measured by M-sequence and sweep frequency methods.

## III. Experiment

The simulations for measuring impedance and sensitivity response curves theoretically verifies that M-sequence method is as effective as the sweep frequency method, but it requires only few milliseconds as well as low power, which is efficient for field test and more suitable for wireless measurement. Moreover, no expensive equipment is required with the proposed approach. In this part, M-sequence signal is generated and analyzed, then the proposed method is employed in a commercial sensor and a recently-developed wireless sensor.

### *A. The M-sequence signal generation*

With the help of a virtual oscilloscope (PicScope, 3206D), the M-sequence signal could be generated and measured simultaneously. Fig. 9. shows two sets of the 11-stage M-sequence in time domain and frequency domain, which measurement bands are 100 kHz and 200 kHz. According to Eq. (5), the clock frequencies of the two M-sequence sets would be 300 kHz and 600 kHz, so the one cycle time will be respectively 6.823 ms and 3.411 ms. Furthermore, the repeatability of the M-sequence is very good, so measuring several cycles of the M-sequence and calculating the average could effectively decrease the deviation of the result.

In conclusion, the larger the measurement band ($f_m$) of M-sequence is, the less time the M-sequence method would take, but the performance requirements for the DAC and the ADC will be higher.

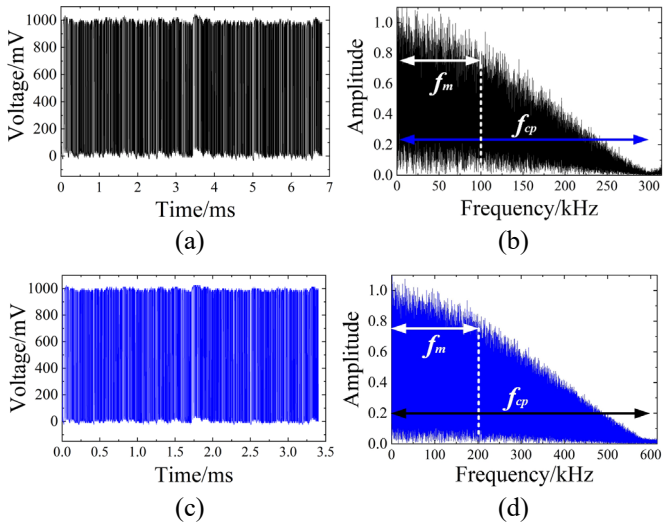


Fig. 9. The generated M-sequence signal. (a) The M-sequence when $f_m$=100 kHz. (b) The normalized power spectrum. (c) The M-sequence when $f_m$=200 kHz. (d) The normalized power spectrum.

### *B. The application on commercial AE sensor*

The experiment setup is shown in Fig. 10. The virtual oscilloscope is controlled by the PC to generate M-sequence signal, sweep frequency signal, and to measure signals from the SUT and the RS. A pincer is employed to fix the two sensors which are protected by two sponges. The coupling agent could increase the AE transmission efficiency. Additionally, for better comparison, the results of impedance analyzer and product data sheet are employed for reference.

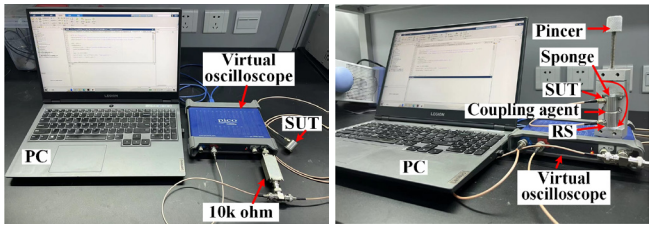


Fig. 10. The calibration experiment setup of commercial AE sensor. (a) Impedance response calibration. (b) Sensitivity response calibration.

The impedance response and sensitivity response curves could be calculated according to Eq. (6) and Eq. (7), and the results are displayed in Fig. 11 (a) and (b). The impedance response curves decrease from about 23 kΩ to 3 kΩ, because the piezoelectric element in AE sensor could be considered as a capacitor. The $R^2$ between impedance response curves of M-sequence method and impedance analyzer is 0.9977, and that of sweep frequency method and impedance analyzer equals 0.9951. On the other hand, the sensitivity response curves overlap well above -90 dB. While under -90 dB, the value is small which could cause error, so the curves deviate. The $R^2$ between impedance response curves of M-sequence method

and product data sheet is 0.956, and that of sweep frequency method and product data sheet equals 0.995.

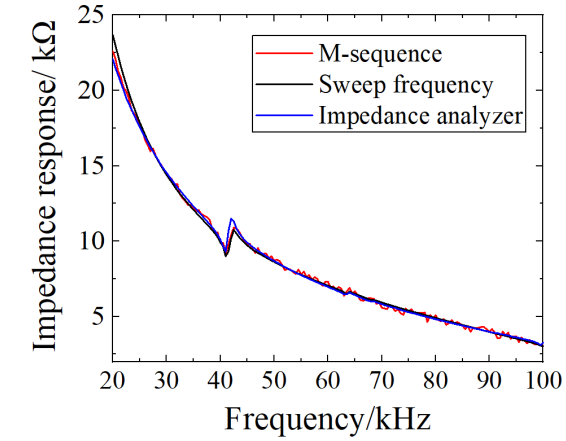


(a)

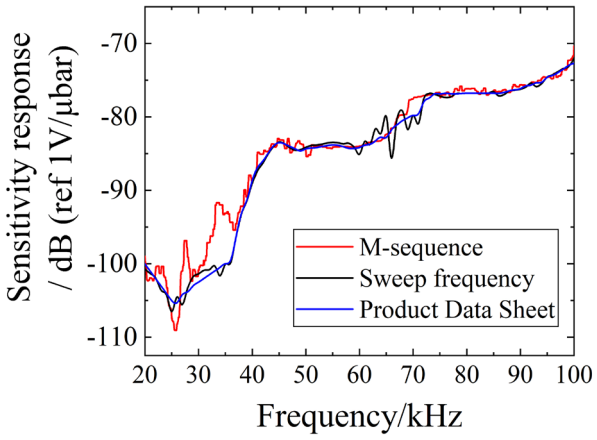


(b)

Fig. 11. The calibration results. (a) Impedance response curve. (b) Sensitivity response curve.

In TABLE II, the M-sequence method and conventional sweep frequency method are compared from aspects of accuracy, consumption and complexity. The accuracy is described by parameter $R^2$, and the costs are measured based on single calibration process. Specifically, the power cost ($P$) and energy cost ($E$) are calculated by Eq. (11) and Eq. (12):

$$P = \frac{1}{t}\int_0^t \frac{u^2(t)}{Z(f)}dt = \frac{1}{t \cdot Z(f)}\int_0^t u^2(t)dt \tag{11}$$

$$E = \int_0^t \frac{u^2(t)}{Z(f)}dt = \frac{1}{Z(f)}\int_0^t u^2(t)dt \tag{12}$$

where $t$ denotes the time required for a single calibration process, $Z(f)$ represents the sensor impedance, $u(t)$ is the excitation signal applied on the sensor. In this paper, the amplitudes of M-sequence signal and sweep frequency signal are both 1 V.

Regarding the M-sequence method, it consumes 6.823 ms for a single calibration, since the sampling frequency is 1 MHz, the frequency resolution would be about 147 Hz. As for the sweep frequency method, to make the comparison convenient, it is set from 20 kHz to 100 kHz by 147 Hz. Considering signal generation performance of the virtual oscilloscope, each frequency signal needs a duration of 1 ms to stabilize the output, the time cost is measured to be around 780 ms. Therefore, although the average power costs of the two methods are consistent, the energy costs are different. The sweep frequency method consumes 390/$Z(f)$ mJ, which is 114 times more than the M-sequence method.

TABLE II
THE COMPARISON BETWEEN THE M-SEQUENCE & SWEEP FREQUENCY METHODS FOR SINGLE CALIBRATION

| Items\methods | M-sequence | Sweep frequency |
|---|---|---|
| Accuracy /$R^2$ factor | Impedance:0.9977 | Impedance: 0.9951 |
| | Sensitivity: 0.956 | Sensitivity: 0.995 |
| Time cost/ms | 6.823 | 780 |
| Average power cost/W | 0.5/$Z(f)$ | 0.5/$Z(f)$ |
| Energy cost/mJ | 3.41/$Z(f)$ | 390/$Z(f)$ |
| Generating complexity | Binary signal (0 or 1) | Continuous signal |

Furthermore, the generating complexity is another apparent advantage of the M-sequence signal, it could be easily generated by binary pulse generator, such as a GPIO (General-Purpose Input/Output) pin, whereas sweep frequency signal can only be produced by a standard signal generator.

### C. *The application on developed wireless sensor*

With the advantages of the proposed method, the authors apply the M-sequence self-calibration in a recently-developed vibration and AE combined wireless sensor.

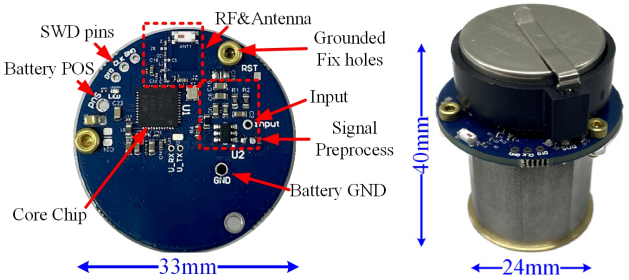


(a) (b)

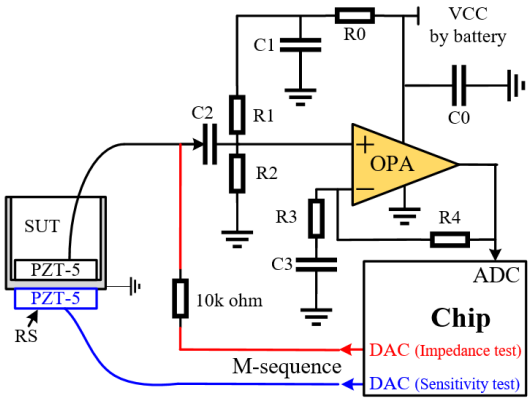


(c)

Fig. 12. The self-calibration applied in wireless sensor. (a) The designed PCB. (b) The designed sensor. (c) Measurement circuit.

The designed Printed Circuit Board (PCB) and wireless sensor prototype are shown in Fig. 12 (a) and (b), while the measurement analog circuit is depicted in Fig. 12 (c). The circuit is designed around the EFR32MG24 System-on-Chip (Silicon Labs) featuring a 32 bit ARM microcontroller and a 2.54 GHz radio transceiver. The red line is used to measure impedance response curve, and the blue line is used to acquire sensitivity response curve. The operation amplifier and related components are responsible for the signal amplification, impedance matching and voltage range shift so that the weak signal provided by the PZT-5 can be properly acquired by the integrated Analog-to-Digital Converter (ADC) on chip.

The M-sequence signal is generated by using the DAC integrated in the microcontroller. It is estimated that the power consumption of DAC would be only 10 mW according to technical manual of the employed chip. In addition, since the $f_{cp}$ of M-sequence is 300 kHz, the sampling rate of ADC should be set at least 600 kHz according to Nyquist theory. The sampling rate is set at 1 MHz in this paper.

To compare the result of M-sequence method with that of standard measurement method, impedance and sensitivity response curves of the sensor are calibrated through impedance analyzer HIOKI IM3590 (sweep frequency) and AE calibration platform (Fig. 13) established according to ISO standard [14].

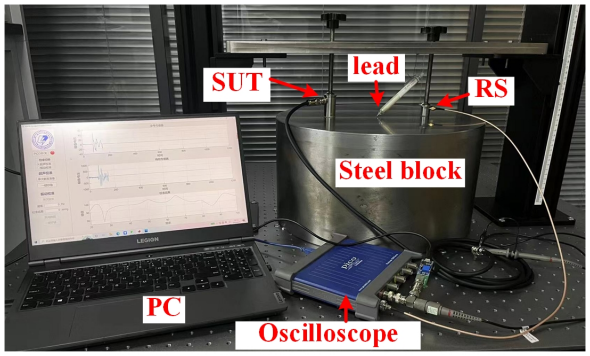


Fig. 13. AE sensitivity response calibration platform(Standard measurement).

Fig. 14 (a) shows that impedance response curves measured by standard measurement and M-sequence method, decreasing from 6 kΩ to 500 Ω, are very similar, although the latter is characterized by small additional fluctuation. The $R^2$ for the two impedance response curves is calculated to be 0.99. Fig. 14 (b) compares the sensitivity response curves from standard measurement and M-sequence method, they coincide very well overall, but differ slightly at some resonant frequencies due to the different experiment conditions (no steel block is employed for M-sequence). The $R^2$ for the two sensitivity response curves is calculated to be 0.986.

The experiment demonstrates M-sequence method is feasible in impedance and sensitivity response calibration, meanwhile, it consumes a relative low energy with a test duration of few milliseconds. Moreover, the calibration does not require any additional device, due to the use of the integrated ADC and DAC which are already available on the microcontroller, thus further reducing cost and size of the final smart sensor. This solution could be applied potentially in smart wireless distributed measurement which contributes to industrial power equipment condition monitoring and evaluation.

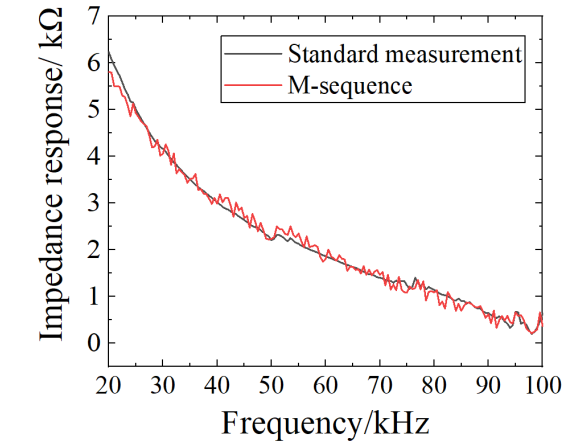


(a)

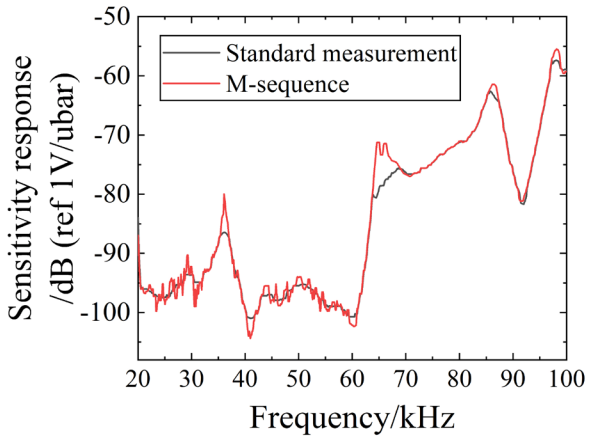


(b)

Fig. 14. The calibration results of M-sequence and standard measurement. (a) Impedance response curve. (b) Sensitivity response curve.

## IV. Conclusion

This paper presents a fast and accurate calibration method excited by M-sequence signal to acquire the impedance and the sensitivity curves of piezoelectric sensor with low cost and power consumption.

M-sequence signal could be designed by the linear feedback shift registers, the clock pulse frequency of M-sequence determines the measurement bandwidth. The feasibility of the method is verified by electrical circuit and FEA simulations, and the achieved results are very promising: the calibration curves obtained by the proposed method almost totally overlap to those obtained by the sweep frequency method. The calibration costs only few milliseconds with about 10 mW of power consumption. On-field tests carried out with commercial AE sensors and recently-designed wireless smart sensor confirm the excellent results of simulations. In particular, no external or additional device is required for the self-calibration since both the ADC and the DAC are already available in the microcontroller of the developed sensor. Therefore, impedance and sensitivity response curves could be self-calibrated at

virtually no additional cost or increase in sensor size.

This work provides a novel, convenient and efficient solution for self-calibration of piezoelectric sensor. In the future, our study will focus on self-calibration excited by M-sequence for the micro-electromechanical systems (MEMS). It can be expected that the impedance and the sensitivity information in frequency domain of the sensors will be acquired rapidly and accurately with very low cost and power.

## REFERENCES


[1] H. D. Ilkhechi and M. H. Samimi, "Applications of the Acoustic Method in Partial Discharge Measurement: A Review," in IEEE Transactions on Dielectrics and Electrical Insulation, vol. 28, no. 1, pp. 42-51, February 2021.

[2] L. Tang, X. Liu, X. Wu and Z. Wang, "An Acoustic Emission Event Filtering Method for Low-Speed Bearing Outer Race Defect Localization," in IEEE Sensors Journal, vol. 22, no. 16, pp. 16293-16305, 15 Aug.15, 2022.

[3] S. Wu, F. Zhang, Y. Dang, C. Zhan, S. Wang and S. Ji, "A Mechanical-Electromagnetic Coupling Model of Transformer Windings and its Application in the Vibration-Based Condition Monitoring," in IEEE Transactions on Power Delivery, vol. 38, no. 4, pp. 2387-2397, Aug. 2023.

[4] M. Zafarani, B. H. Jafari and B. Akin, "Lateral and Torsional Vibration Monitoring of Multistack Rotor Induction Motors," in IEEE Transactions on Industrial Electronics, vol. 68, no. 4, pp. 3494-3505, April 2021.

[5] M. Iorgulescu, R. Beloiu and M. O. Popescu, "Vibration monitoring for diagnosis of electrical equipment's faults," 2010 12th International Conference on Optimization of Electrical and Electronic Equipment, 2010, pp. 493-499.

[6] S. Wang, J. Shan, H. Tian and S. Lin, "The High-Power Piezoelectric Transformer With Multiple Outputs Based on Sandwiched Piezoelectric Transducers, " in IEEE Transactions on Power Electronics, vol. 37, no. 8, pp. 8886-8894, Aug. 2022.

[7] S. -T. Yun and S. -H. Kong, "Design of High Efficiency Controller for Wide Input Range DC-DC Piezoelectric Transformer Converter," in IEEE Access, vol. 8, pp. 225650-225662, 2020.

[8] J. Zhao, Y. Huang, X. Wen, S. Zhang and P. Liu, "Identification of Geometric Parameters Influencing the Impedance Sensitivity of Piezoelectric Mass Sensors," in IEEE Sensors Journal, vol. 20, no. 24, pp. 14740-14746, 15 Dec.15, 2020.

[9] Sukesha, R. Vig and N. Kumar, "Variation of piezoelectric coefficient and dielectric constant with electric field and temperature: A review," 2014 Recent Advances in Engineering and Computational Sciences (RAECS), Chandigarh, India, 2014, pp. 1-6.

[10] Janů P, Bajer J, Dyčka P, et al. "Precise experimental determination of electrical equivalent circuit parameters for ultrasonic piezoelectric ceramic transducers from their measured characteristics," Ultrasonics, 2021, 112: 106341.

[11] Z. Zhang et al., "A Novel IEPE AE-Vibration-Temperature-Combined Intelligent Sensor for Defect Detection of Power Equipment," in IEEE Transactions on Instrumentation and Measurement, vol. 72, pp. 1-9, 2023, Art no. 9506809.

[12] Methods for the calibration of vibration and shock transducers - Part 21: Vibration calibration by comparison to a reference transducer, ISO 16063-21:2003.

[13] Y. -y. Wang, L. -b. He, H. -j. Zhu and P. Yang, "Consistency of surface pulse and reciprocity calibration of piezoelectric AE sensors," 2015 Symposium on Piezoelectricity, Acoustic Waves, and Device Applications (SPAWDA), Jinan, China, 2015, pp. 189-192.

[14] Non-destructive testing-Acoustic emission inspection-Secondary calibration of acoustic emission sensors, ISO 12714:1999.

[15] Non-destructive testing-Acoustic emission inspection-Primary calibration of acoustic emission sensors, ISO 12713:1998.

[16] Non-destructive testing - Methods for absolute calibration of acoustic emission transducers by the reciprocity technique, ISO/TR 13115-2011.

[17] H. Hatano, T. Chaya, S. Watanabe and K. Jinbo, "Reciprocity calibration of impulse responses of acoustic emission transducers," in IEEE Transactions on Ultrasonics, Ferroelectrics, and Frequency Control, vol. 45, no. 5, pp. 1221-1228, Sept. 1998.

[18] Lan H, Yan L, Xiao D, et al. "Surface-to-surface calibration of acoustic emission sensors," Sensors and Actuators A: Physical, 2012, 174: 16-23.

[19] L. Zhang, Hazim Yalcinkaya, and Didem Ozevin, "Numerical approach to absolute calibration of piezoelectric acoustic emission sensors using multiphysics simulations," Sensors and Actuators A: Physical, vol. 256, pp. 12–23, Apr. 2017.

[20] M. A. Jamshed, K. Ali, Q. H. Abbasi, M. A. Imran and M. Ur-Rehman, "Challenges, Applications, and Future of Wireless Sensors in Internet of Things: A Review," in IEEE Sensors Journal, vol. 22, no. 6, pp. 5482-5494, 15 March15, 2022.

[21] V. C. Gungor, B. Lu and G. P. Hancke, "Opportunities and Challenges of Wireless Sensor Networks in Smart Grid," in IEEE Transactions on Industrial Electronics, vol. 57, no. 10, pp. 3557-3564, Oct. 2010.

[22] Pertijs M. "Calibration and Self-Calibration of Smart Sensors," Smart Sensor Systems: Emerging Technologies and Applications, 2014: 17-41.

[23] U. Guner and J. Dasdemir, "Novel Self-Calibration Method for IMU Using Distributed Inertial Sensors," in IEEE Sensors Journal, vol. 23, no. 2, pp. 1527-1540, 15 Jan.15, 2023.

[24] Y. Chen, L. Du, Q. Sun, J. Bai, H. Li and Y. Shi, "Self-Calibration Method of Displacement Sensor in AMB-Rotor System Based on Magnetic Bearing Current Control," in IEEE Transactions on Industrial Electronics, vol. 71, no. 5, pp. 5148-5156, May 2024.

[25] M. Pertijs, "Calibration and self-calibration of smart sensors" in Smart Sensor Systems: Emerging Technologies and Applications, Hoboken, NJ, USA:Wiley, pp. 17-41, 2014.

[26] T. Yan, P. Theobald, and B. E. Jones, "A conical piezoelectric transducer with integral sensor as a self-calibrating acoustic emission energy source," Ultrasonics, vol. 42, no. 1–9, pp. 431–438, Apr. 2004.

[27] L. Yanjun, and Z. Ke, System Identification Theory and Application, National Defense Industry Press: Beijing, 2009, ch.2.

[28] Y. Luo, J. Gao, P. Chen, L. Hu, Y. Shen and L. Ruan, "A test method of winding deformation excited by pseudorandom M-Sequences — Part I: Theory and simulation," in IEEE Transactions on Dielectrics and Electrical Insulation, vol. 23, no. 3, pp. 1605-1612, June 2016.

[29] Chien-Yi Chen, Cheng-Chi Tai, Ching-Chau Su, Ju-Chu Hsieh and Jiann-Fuh Chen, "GIS partial discharge examination and classification from the on-line measurements," 2008 International Conference on Condition Monitoring and Diagnosis, 2008, pp. 412-415.



**Zhaoyu Zhang**, was born in Yuncheng, Shanxi, China, in 1995. He received the M.S. degree in electrical engineering from Xi'an Jiaotong University, Xi'an, in 2020. He is currently pursuing the double Ph.D. degree in electrical engineering with Xi'an Jiaotong University, Xi'an, China and Politecnico di Torino, Turin, Italy. His main fields of interest are the intelligent sensing technology, fault detection and state evaluation for power equipment.



**Tianyi Shi** was born in 2000. He received the B.Sc. degree in electrical engineering from Xi'an Jiaotong University, Xi'an, in 2022, where he is currently pursuing the M.S. degree with a focus on the intelligent sensing technology, fault detection and state evaluation for power equipment.

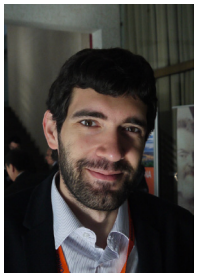

**Luca Lombardo** (Member, IEEE) received the B.S. degree and the M.S. in Electronic Engineering, respectively, in 2014 and 2016 from the University of Messina, Messina (Italy). He received the Ph.D. degree in Metrology from the Politecnico di Torino, Turin (Italy) in 2019. He is Assistant Professor in the measurement and instrumentation field with the Department of Electronics and Telecommunications at Politecnico di Torino, Turin (Italy). His research interests includes the development of innovative sensors and systems, embedded systems and measurement instrumentation, especially in the fields of environmental monitoring, biomedical applications and cultural heritage

**Yidan Hu** was born in Henan, China, in 1995. She received the M.S. degree from North China Electric Power University, Beijing, China, in 2019. She is currently pursuing the double Ph.D. degree in electrical engineering with Xi'an Jiaotong University, Xi'an, China and Politecnico di Milano, Milan, Italy.

**Haotian Wang** was born in Xi'an, Shaanxi, China, in 1999. He received the B.Sc. degree in electrical engineering from Xi'an Jiaotong University, Xi'an in 2020, where he is currently pursuing the Ph.D. degree with a focus on the fault detection and state evaluation for gas-insulated switchgear equipment.

**Xuanrui Zhang** was born in Zhengzhou City, Henan Province, China in 1994. He received the Ph.D degree Xi'an Jiaotong University, Xi'an, China in 2023. Currently, he is an Assistant Professor at Xi'an Jiaotong University. He focuses on the partial discharge detection and impulse test technology for power transformers.

**Marco Parvis** (Fellow, IEEE) was born in Italy, in 1958. He received the M.S. degree in electrical engineering and the Ph.D. degree in metrology from the Politecnico di Torino, Turin, Italy, in 1982 and 1987, respectively. He is currently a Full Professor of electronic measurements with the Politecnico di Torino, where he was the Dean of the II Faculty of Engineering. His main fields of interest are intelligent instrumentation, application of signal processing to measurement, biomedical, and chemical measurements. He has authored more than 100 publications.

**Junhao Li** (Senior Member, IEEE) was born in Xuchang, Henan, China, in 1980. He received the Ph.D. degree in electrical engineering from Xi'an Jiaotong University, Xi'an, China, in 2010.

He is currently a Professor with Xi'an Jiaotong University, where he is involved in the detective and diagnostic techniques for electrical equipment and new types of the test method for electrical equipment, etc.